Hall-Velocity Limited Magnetoconductivity in a Classical Two-Dimensional Wigner Crystal

A. Kristensen, K. Djerfi, P. Fozooni, M. J. Lea, P. J. Richardson, and A. Santrich-Badal
Department of Physics, Royal Holloway, University of London, Egham, Surrey TW20 0EX, England

A. Blackburn
Department of Electronics and Computer Science, University of Southampton, Southampton SO17 1BJ, England

R. W. van der Heijden
Department of Physics, Eindhoven University of Technology, NL 5600 MB Eindhoven, The Netherlands
(Received 28 December 1995; revised manuscript received 30 May 1996)

The magnetoconductivity $\sigma_{xx}(B)$ of a classical two-dimensional electron crystal on superfluid ^{4}He is nonlinear. Experimentally, we find a contribution to $\sigma_{xx}(B)$ which, at constant field B, gives $\sigma_{xx}(B) \propto J_x$, the current density, while at constant current, $\sigma_{xx}(B) \propto 1/B$. For increasing J_x, the Hall velocity v_H slowly approaches the ripplon velocity v_l at the first reciprocal lattice vector, due to strong electron-ripplon interactions with the helium. The magnetoconductivity then decreases sharply for $v_H > v_1$. [S0031-9007(96)00837-X]

PACS numbers: 73.20.Dx, 67.90.+z, 73.50.Jt

Electrons in surface states above bulk superfluid helium form the simplest conducting system known experimentally [1]. They interact strongly and, at low temperatures, form a classical two-dimensional (2D) electron solid, the Wigner crystal. This was first detected [2] from the onset of coupled-plasmon ripplon (CPR) mode resonances [3] below the transition temperature T_m, which occurs at a value of the plasma parameter $\Gamma_m = 127 \pm 3$ (the ratio of the potential and kinetic energies) [4,5]. These modes arise from interactions between the electrons and ripplons which have been considered to produce a coherent deformation, or dimple, in the helium surface beneath each electron [5,6]. This crystal has been particularly important for the study of 2D melting and the Kosterlitz-Thouless transition [4], though the exact nature of the melting transition in 2D systems and even the order of the transition is still controversial [7]. Ryzkov and Tareyeva [8] have recently considered the interaction potentials for which melting should involve two continuous transitions from the solid to the fluid via the hexatic phase, as previously proposed [4]. In zero magnetic field the crystal is an excellent conductor, with an electron mobility μ as high as 800 m^2/Vs for an electron density of 1.05×10^{12} m^{-2} [9]. Until recently, little was known about the magnetoconductivity $\sigma_{xx}(B) = \sigma(B)$ in a magnetic field B. Giannetta and Wilen [10] found hysteresis in the solid phase in a magnetic field which they interpreted as shear induced melting in crossed electric and magnetic fields. Shirahama and Kono [11] have further studied this hysteresis in the magnetoconductivity in the solid and interpret it as a dynamical transition in which the electrons collectively slide out of the periodic deformation of the He surface about some threshold value of the excitation voltage to form a solid without CPR modes. Below the threshold, $\sigma(B)$ is also nonlinear and has a distinctive field dependence $1/\sigma(B) \propto B$ [11,12] in contrast to the Drude behavior $1/\sigma(B) \propto B^2$ observed in the fluid phase [13]. We now present new measurements of $\sigma(B)$ in the 2D Wigner crystal on helium in the low drive region below the threshold. We find that, as the excitation increases, the Hall drift velocity in the crossed electric and magnetic fields approaches a limiting value close to the ripplon velocity at the first reciprocal lattice vector of the crystal. This leads to the nonlinear magnetoconductivity with excitation voltage and the frequency and field dependences found experimentally. Above the threshold in the solid, the Hall velocity increases sharply. Nonlinear behavior is also a crucial feature of the metal-insulator transition in the 2D electrons in GaAs/AlGaAs heterostructures, which has usually been attributed to the formation of a pinned Wigner crystal, but may actually be a percolation metal-insulator transition [14]. The classical 2D electron solid on helium is the clearest experimental example of a 2D Coulomb solid.

The magnetoconductivity of 2D electrons above superfluid helium was measured using a Corbino disk a distance d (typically 100 μm) beneath the helium surface [13] as shown in Fig. 1. A central electrode A (radius $r_1 = 1.2$ mm) is surrounded by a ring E (outer radius $r_3 = 1.4$ mm) which separates the receiving electrodes B1, B2, and B3 (outer radius $r_2 = 2.0$ mm). Around these is a planar guard G. The electrode separation is 10 μm. Free electrons were held in place by dc potentials on electrodes A, B, and E (ground), the guard electrode G $(-ve)$ and a top plate $(-ve)$ at $h = 1.6$ mm above the electrodes. The electron density n was determined from the $-ve$ dc bias voltage on electrode E required to cut off the ac current between electrodes A and B. An ac voltage V_0 from 1 to 500 mV rms at a frequency $f = \omega/2\pi$ between 1 and 50 kHz was applied to electrode A and the ac currents I to the electrodes B were measured. For a perfect conductor the phase of the capacitively coupled

 0031-9007/96/77(7)/1350(4)$10.00

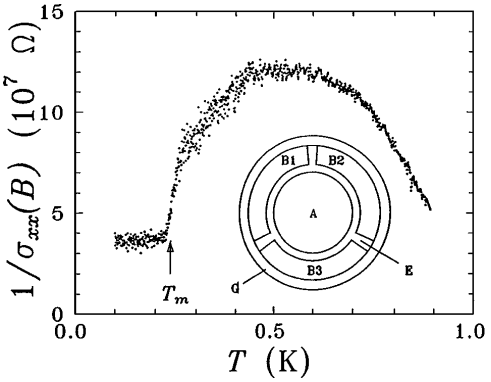

FIG. 1. The temperature dependence of $1/\sigma(B)$ for $n = 1.2 \times 10^{12}$ m^{-2}, $B = 0.2$ T, $f = 7$ kHz, and $V_0 = 10$ mV rms, showing the transition to the solid phase at $T_m = 0.24$ K. Inset: Corbino disk geometry.

current I is $\pi/2$ with respect to V_0. The phase shift $\phi(B)$ away from $\pi/2$ in a perpendicular magnetic field is proportional to $1/\sigma(B)$ for $\phi \leq 0.3$ rad [15], while for larger phase shifts the theoretical response function was used to evaluate $1/\sigma$ from ϕ.

The magnetoconductivity was measured as a function of temperature, excitation voltage, frequency, and magnetic field for a range of electron densities in the fluid and solid phases. The temperature dependence of $1/\sigma(B)$ in a perpendicular magnetic field $B = 0.2$ T for a drive of 10 mV is shown in Fig. 1 for $n = 1.2 \times 10^{12}$ m^{-2}. The inverse magnetoconductivity increases below 1 K with the mobility, as $1/\sigma(B) \approx \mu B^2/ne$ (the Drude model) in this region. A sharp transition to the electron solid phase is observed at $T_m = e^2(\pi n)^{1/2}/4\pi\overline{\varepsilon}\varepsilon_0 k_B \Gamma_m = 0.225 \times 10^{-6} n^{1/2}$K where $\overline{\varepsilon} = (1 + \varepsilon)/2$ [5], below which the conductivity is almost independent of temperature.

In the fluid phase, only a small nonlinearity is found as $\sigma(B)$ decreases quadratically with drive voltage (by $\leq$20% for $V_0 \leq 100$ mV), which may be due to hot-electron effects [16]. However, the behavior in the solid phase is strikingly different as shown in Fig. 2 where $\sigma(B)$ is plotted versus V_0 at 0.06 K for $B = 0.2$ T for a measurement frequency of 4 kHz for several electron density. At low voltages, the magnetoconductivity $\sigma(B)$ increases almost linearly up to a threshold voltage V_c where it decreases rapidly. No hysteresis was observed, in contrast to Shirahama and Kono [11].

This nonlinearity strongly depends on the measurement frequency used and on the magnetic field as shown in Fig. 3, where $\sigma(B)$ is plotted for several frequencies in a fixed magnetic field and in Fig. 4 for several fields at a fixed frequency. The general features are the same in each case but the rate of increase of $\sigma(B)$ with drive voltage increases for higher frequencies and lower magnetic fields.

The consequences of these measurements are quite remarkable. The excitation voltage is capacitively coupled and, for small phase shifts, this corresponds to a current

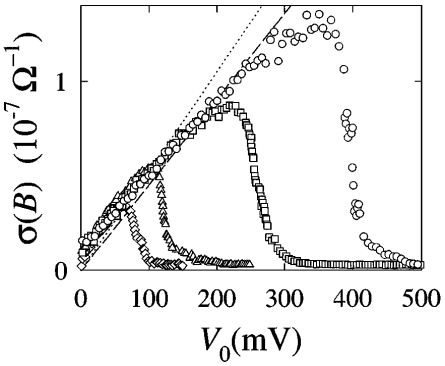

FIG. 2. The magnetoconductivity $\sigma(B)$ for $n = 1.06 \times 10^{12}$ ($\diamond$), 1.20×10^{12} ($\triangle$), 1.57×10^{12} ($\square$), and 1.90×10^{12} m^{-2} ($\bigcirc$) at 0.06 K, $B = 0.2$ T, $f = 4$ kHz versus the rms excitation voltage V_0. The conductivities from Eq. (1) are shown with $v_H = v_1 = 4.09$ m/s ($n = 1.06 \times 10^{12}$ m^{-2}, dotted line) and $v_1 = 4.74$ m/s ($n = 1.90 \times 10^{12}$ m^{-2}, dashed line).

bias with an rms radial current density over the Corbino disk, $J = CfV_0/d = (1.24 \times 10^{-14} fV_0)/d$ A/m where the constant C depends on the electrode geometry. If we have $\sigma(B) \propto V_0$ then, since $\sigma_{xx}E_x = J_x \propto V_0$, the electric field E_x would be independent of V_0. A simple explanation is suggested from the motion of electrons in crossed electric and magnetic fields. The cyclotron orbits acquire a drift velocity v_x along the electric field but also move at right angles to it with a Hall velocity $v_H = E_x/B$ (for both classical and quantum orbits if $\omega_c\tau \gg 1$, where τ is the scattering time; these experiments are close to the quantum region $\hbar\omega_c/kT = 1.344B/T > 1$). Hence

$$\sigma(B) = \frac{J_x}{E_x} = \frac{J_x}{v_H B} = \frac{CfV_0}{v_H B d}. \qquad (1)$$

We can therefore calculate the experimental rms value of $v_H = CfV_0/\sigma(B)Bd$ as shown in Fig. 5 for the data from Fig. 2 at different densities. As V_0 increases the Hall velocity slowly increases towards a limiting value of between 4 and 5 m/s. Above this critical velocity

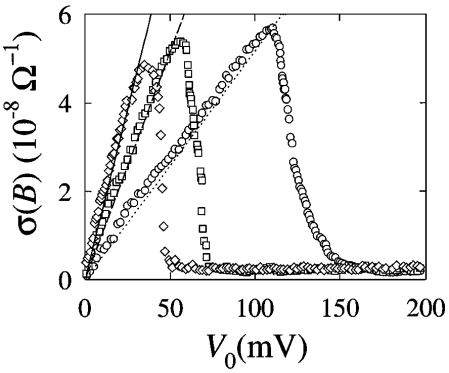

FIG. 3. The magnetoconductivity $\sigma(B)$ versus the rms excitation voltage V_0 for $n = 1.13 \times 10^{12}$ m^{-2} at 0.07 K, $B = 0.2$ T, for $f = 4$ ($\bigcirc$), 8 ($\square$), and 12 ($\diamond$) kHz. The lines show the conductivities from Eq. (1) with $v_H = v_1 = 4.1$ m/s.

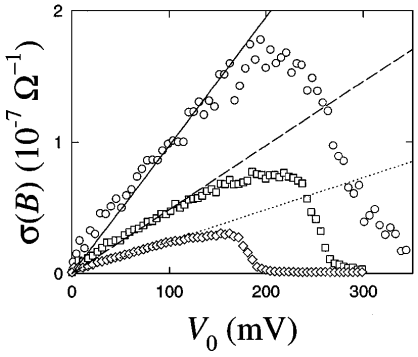

FIG. 4. The magnetoconductivity $\sigma(B)$ versus the rms excitation voltage V_0 for $n = 1.44 \times 10^{12}$ m^{-2} at 0.07 K, for $f =$ 4 kHz and $B = 0.1$ (○), 0.2 (□), and 0.4 (◇). The lines show the conductivities from Eq. (1) with $v_H = v_1 = 4.3$ m/s.

the Hall velocity increases rapidly. For linear conduction $\sigma(B)$ would be independent of V_0 while v_H would be proportional to V_0.

These critical velocities suggests the underlying physics. The shallow dimple beneath each electron can be expanded as a Fourier series in the reciprocal lattice vectors $G_p^2 = pG_1^2$ of the crystal [3,5,6] for $p = 1, 3, 4, 7, 9$, etc. with $G_1 = 2\pi(2/\sqrt{3})^{1/2}n^{1/2}$. As the electrons and dimples are driven at a velocity $v \approx v_H$, the helium surface will oscillate at frequencies $\omega_p = \boldsymbol{G}_p \cdot \boldsymbol{v}$. This will give a resonant response as ω_p approaches the frequencies of the ripplon modes $\Omega_p = (\alpha/\rho)^{1/2}G_p^{3/2}$ at the reciprocal lattice vectors, where α is the surface tension and ρ the density of the helium. In a field B the coupled magnetoplasmon-ripplon (CPR) modes [5,17] should be at much higher frequencies than Ω_1. This resonance will give a drive dependent drag term in the equation of motion which will increase rapidly as ω_1 approaches Ω_1 and puts an upper limit on the Hall velocity equal to the phase velocity $v_1 = (\alpha G_1/\rho)^{1/2}$ of the ripplons with wave vector G_1 (this *increases* the magnetoconductivity). For the electron densities shown in Figs. 2 and 5, $v_1 = 4.09$, 4.20, 4.52, and 4.74 m/s. The comparison with the data strongly suggests that these are the relevant velocities.

If we now assume that the Hall velocity is constant then Eq. (1) immediately gives all the nonlinear features observed experimentally. The lines in Figs. 2, 3, and 4 show the conductivities calculated from Eq. (1) with $v_H = v_1$. In each case the experimental values are parallel to these lines, below the threshold voltage. Of course the drift and Hall velocities are actually both time and space dependent. Further theoretical work is required.

Another consequence of Eq. (1) is that $1/\sigma(B)$ should increase linearly with magnetic field in the solid if the Hall velocity is limited by the ripplon velocity. In the fluid phase in low magnetic fields, $B \leq 0.3$ T, the magnetoconductivity follows the Drude result

$$\frac{\sigma_0}{\sigma(B)} = 1 + \mu^2 B^2 , \qquad (2)$$

where $\sigma_0 = ne\mu$ is the zero-field conductivity, even though $\mu B \gg 1$ [12]. This behavior is due to many-electron effects: the fluctuating internal electric fields E_f in the electron fluid produce an energy uncertainty eE_fL where L is the de Broglie wavelength, the classical cyclotron radius or the magnetic length. For $\hbar\omega_c < eE_fL$ ($\omega_c = eB/m$ is the cyclotron frequency), or $B < B_0$, an onset field for magnetoresistance, the Landau levels are smeared out and the Drude model applies [13]. The behavior in the solid phase is quite different, with $1/\sigma(B) \propto B$ with a gradient which is drive dependent as shown in Fig. 6 for drive levels of 10, 15, and 30 mV rms. Equation (1) suggests that, in nonlinear region, $\sigma(B)$ should scale as $1/B$, as found experimentally [18].

A closely related model has been given for the critical drift velocity in the quantum Hall regime in a 2D electron gas in semiconducting GaAs/AlGaAs heterostructures [19] using the concept of Landau critical velocity. In the frame of the reference of the drifting electrons (velocity $\boldsymbol{v}$) the change in energy of the ripplons (phonons

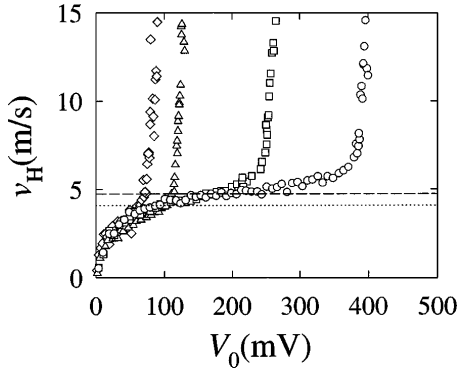

FIG. 5. The rms Hall velocity v_H versus the rms excitation voltage V_0 for the data in Fig. 2 for $n = 1.06 \times 10^{12}$ (◇), 1.20×10^{12} (△), 1.57×10^{12} (□), and 1.90×10^{12} m^{-2} (○) at 0.06 K. The ripplon velocities $v_1 = 4.09$ m/s ($n = 1.06 \times 10^{12}$ m^{-2}, dotted line) and $v_1 = 4.74$ m/s ($n = 1.90 \times 10^{12}$ m^{-2}, dashed line) are shown.

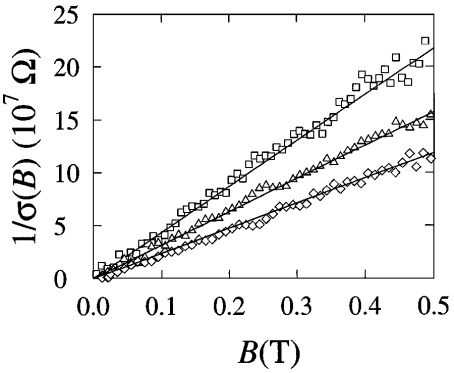

FIG. 6. $1/\sigma(B)$ versus B in the solid phase for $n = 1.1 \times 10^{12}$ m^{-2} at 0.06 K, $f = 4$ kHz for $V_0 = 10$ mV (□), and 15 mV (△) and 30 mV (◇) rms.

in GaAs) due to the creation of an excitation $\varepsilon(\boldsymbol{p})$ of momentum $\boldsymbol{p}$ is $\Delta E = \varepsilon(\boldsymbol{p}) + \boldsymbol{v} \cdot \boldsymbol{p}$. If $|\boldsymbol{v}| > \varepsilon(\boldsymbol{p})/\boldsymbol{p} = \boldsymbol{v}_\phi$, the excitation phase velocity $\Delta E < 0$ and spontaneous emission of ripplons can occur. For the 2D electron crystal, this will be amplified for coherent ripplons at the reciprocal lattice vectors with $\boldsymbol{v}_\phi = \boldsymbol{v}_1$ for G_1.

These ideas also demonstrate another aspect of the dynamical transition observed by Shirahama and Kono [11]. As the Hall velocity increases, there will come a point where the electron breaks loose from its dimple, which then disappears for $v_H > v_1$, as originally suggested by Fisher *et al.* [3] in the first discussion of CPR modes. The third harmonic current increased sharply above the threshold voltage indicating an abrupt mobility change during each cycle.

The effects of electron heating must also be considered. Glattli *et al.* [20] measured the thermal time constant (11 μs at 0.1 K) and the heat capacity ($1.2k_B$ per electron at 0.1 K) for $n = 1.02 \times 10^{12}$ m^{-2} in the solid phase (for $B = 0$) and hence we can estimate the temperature differential ΔT between the electrons and the helium. For the data shown in Fig. 2 the total power input to the electron solid was 4×10^{-14} W giving $\Delta T = 0.002$ K at $V_0 = 10$ mV. Below the threshold voltage, heating effects, $\propto J^2/\sigma$, are relatively small.

We have presented measurements of the nonlinear magnetoconductivity $\sigma(B)$ with excitation voltage and the frequency dependence and the magnetic-field dependence in a classical 2D Wigner electron crystal on superfluid helium. All these features are most unusual but we have shown how they can be simply related by assuming that the Hall velocity v_H is limited to the ripplon velocity v_1 at the first reciprocal lattice vector. Above a *ripplon barrier* at $v_H = v_1$ the magnetoconductivity decreases rapidly.

We thank Professor M. I. Dykman, Dr. J. Saunders, and Dr. G. Deville for useful discussions; Professor K. Kono for sending preprints of his work; the EPSRC (UK) for a Research Grant and for a Studentship (for P. J. R.); the EU for support under Contract No. CHRXCT 930374; A. K. Betts, F. Greenough, and J. Taylor for technical assistance; D. Murphy, A. Jury, and the staff of the Southampton University Microelectronics Centre and the lithography unit of the Rutherford Appleton Laboratory, UK, for electrode fabrication.

[1] For an introductory review, see W. F. Vinen and A. J. Dahm, Phys. Today **40**, 43 (1987).
[2] C. C. Grimes and G. Adams, Phys. Rev. Lett. **42**, 795 (1979).
[3] D. S. Fisher, B. I. Halperin, and P. M. Platzman, Phys. Rev. Lett. **42**, 798 (1979).
[4] D. R. Nelson and B. I. Halperin, Phys. Rev. B **19**, 2457 (1979); A. P. Young, Phys. Rev. B **19**, 1855 (1979); E. Y. Andrei, F. I. B. Williams, D. C. Glattli, and G. Deville, in *The Physics of Low-dimensional Semiconductor Structures*, edited by P. Butcher *et al.* (Plenum Press, New York, 1993), Chap. 14, p. 499.
[5] G. Deville, J. Low Temp. Phys. **72**, 135 (1988).
[6] K. Kono, J. Phys. Soc. Jpn. **56**, 1111 (1987).
[7] K. Chen, T. Kaplan, and M. Mostoller, Phys. Rev. Lett. **74**, 4019 (1995); K. Bagchi, H. C. Andersen, and W. Swope, Phys. Rev. Lett. **76**, 255 (1996).
[8] V. N. Ryzhov and E. E. Tareyeva, Phys. Rev. B **51**, 8789 (1995).
[9] R. Mehrotra, C. J. Guo, Y. Z. Ruan, D. B. Mast, and A. J. Dahm, Phys. Rev. B **29**, 5239 (1984); M. A. Stan and A. J. Dahm, Phys. Rev. B **40**, 8995 (1989).
[10] R. Giannetta and L. Wilen, Solid State Commun. **78**, 199 (1991).
[11] K. Shirahama and K. Kono, Phys. Rev. Lett. **74**, 781 (1995).
[12] P. J. Richardson, A. Blackburn, K. Djerfi, M. I. Dykman, C. Fang-Yen, P. Fozooni, A. Kristensen, M. J. Lea, and A. Santrich-Badal, Surf. Sci. (to be published)
[13] M. J. Lea, P. Fozooni, P. J. Richardson, and A. Blackburn, Phys. Rev. Lett. **73**, 1142 (1994); P. Fozooni, P. J. Richardson, M. J. Lea, M. I. Dykman, C. Fang-Yen, and A. Blackburn, J. Phys. Condens. Matter **8**, L215 (1996).
[14] A. A. Shaskin, V. T. Dolgopolov, G. V. Kravchenko, M. Wendel, R. Schuster, J. P. Kotthaus, R. J. Haug, K. von Klitzing, K. Ploog, H. Nickel, and W. Schlapp, Phys. Rev. Lett. **73**, 3141 (1994).
[15] Experimentally the phase shift ϕ is a well-defined parameter which specifies the losses in the system. We used the standard expression for a Corbino disk [see R. Mehrotra and A. J. Dahm, J. Low Temp. Phys. **67**, 115 (1987)] to obtain values of the magnetoconductivity from ϕ. This is strictly correct for a linear, local, and uniform conductor. In the nonlinear solid phase, this defines an effective magnetoconductivity.
[16] M. Saitoh, J. Phys. Soc. Jpn. **42**, 201 (1977).
[17] D. M. Mast, A. J. Dahm, and A. L. Fetter, Phys. Rev. Lett. **54**, 1706 (1985); D. C. Glattli, E. Y. Andrei, G. Deville, J. Poitrenaud, and F. I. B. Williams, Phys. Rev. Lett. **54**, 1710 (1985).
[18] Equation (2) holds only for $\hbar\omega_c/kT < 1$ ($B < 0.07$ T at 0.1 K). A field independent scattering time for $\hbar\omega_c/kT > 1$ would give $1/\sigma(B) \propto B$, as the diffusion length becomes the magnetic length $l = (\hbar/eB)^{1/2}$ (quantum Drude model), but with no intrinsic drive or frequency dependence.
[19] P. Streda and K. von Klitzing, J. Phys. C **17**, L486 (1984).
[20] D. C. Glattli, E. Y. Andrei, and F. I. B. Williams, Surf. Sci. **196**, 17 (1988).